

## Soil properties at the UCD geotechnical research site at Blessington

Paul Doherty<sup>1</sup>, Lisa Kirwan<sup>1</sup>, Kenneth Gavin<sup>1</sup>, David Igoe<sup>1</sup>, Shane Tyrrell<sup>2</sup>, Darren Ward<sup>3</sup>, Brendan O'Kelly<sup>4</sup>  
<sup>1</sup>School of Civil, Structural and Environmental Engineering, University College Dublin, Belfield, Dublin, Ireland  
<sup>2</sup>Department of Geology, University College Dublin, Belfield, Dublin, Ireland  
<sup>3</sup>In-situ Site Investigations, Penetration House, UK  
<sup>4</sup>Department of Civil, Structural and Environmental Engineering, Trinity College Dublin  
 email: paul.doherty@ucd.ie

**ABSTRACT:** Over the past ten years, the Geotechnical Research Group (GRG) at University College Dublin have developed a research site at Blessington, County Wicklow, for the purpose of testing foundation systems. This paper presents the results of field and laboratory tests conducted to obtain the geotechnical parameters of Blessington sand. The in-situ tests included cone penetration and dilatometer tests. Sonic coring was performed in three boreholes at the site and complete recovery was obtained in boreholes up to 14 m deep. Additional disturbed samples were taken from trial pits which were up to 6 m deep. The classification tests performed on samples compared favourably with those inferred from correlations with in-situ test data. The strength, stiffness and mineralogy were also determined by a suite of laboratory tests including SEM imagery, triaxial tests and ring shear testing. The accuracy of conventional correlations in predicting the laboratory measured parameters is discussed.

**KEY WORDS:** Soil testing, soil classification, mineralogy

### 1 INTRODUCTION

Over the past ten years, the geotechnical research group (GRG) at University College Dublin have developed a field testing facility at Blessington, County Wicklow (see [1]). This test site was developed to accommodate a series of research projects, which investigated aspects of foundation behaviour including axial pile behaviour, lateral pile resistance, cyclic loading response, eccentric loading and pile ageing. This test site was chosen because of the consistent nature of the sand deposits and the similarity of the strength and stiffness properties of the sand to those encountered in offshore seabed deposits in the North Sea.

This paper compiles data from site characterisation testing that has been undertaken to-date and combines this to develop a holistic interpretation of the test site properties.

### 2 TEST SITE LOCATION

The Blessington test site is located in the Redbog Roadstone quarry approximately 25km south-west of Dublin, see Figure 1. The site access is approximately 800m to the north-west of Blessington village, comprises of an area of approximately 30m x 30m, and consists of uniform dense sand from ground surface to considerable depth.

Over the years in which experimental work has been performed on the test site, excavation has proceeded in adjacent areas, and the test area now occupies an elevated position (See Figure 2). These excavations and recently completed sonic coring provided an opportunity to sample the sand from much greater depths than had been possible previously.

### 3 SITE GEOLOGY

#### 3.1 Geological History

The geological history of the area has been investigated by a number of researchers (eg. [2]), who describe the complex

glacial movements that formed the underlying sand deposits. The sediments of the Blessington sand and gravel pits represent the deposits of a lacustrine delta complex (where sediment carried by a river is deposited as the water slows down as it flows into a lake), with the envisaged glacial lake impounded by the Midlandian ice sheet to the west and by the Wicklow Mountains to the east. The sediments, locally underlain by slates and shale of Silurian age, have a maximum thickness of 60 m, but the exact age of these deposits is uncertain. Divided into two phases of deposition, the earlier stage (part of which forms the site area investigated in this study) is linked to the retreat of the ice sheet; hence was likely bracketed between 20–24 kiloannum (ka) (the maximum extent of the sheet) and a later ice re-advance dated at 17 (ka) [3].



Figure 1. Blessington test site location.



Figure 2. Excavations at Blessington test site (after [4]).

The complex is comprised of a frequently contorted sequence of dominantly gravelly to coarse- to medium-grained sand beds and facies associated with a typical Gilbert-type delta (a specific type of delta characterised by predominantly coarse sediments). However, the site investigation is specifically focused on a relatively well-sorted, fine- to medium-grained sand facies. The sediments at the test site correspond to the Light Brown Unit, described by Philcox [5], and form the uppermost part of a significant local fluvial channel system. Comprising horizontal, interlaminated (5–15 cm scale), rippled cross-laminated sands and silts, these sediments represent the deposits of a low energy fluvial current.

A later, but limited, ice re-advance (associated with the 17 ka event) was likely to have covered the study area, the final retreat of which resulted in the deposition of a minimum of 7 m overburden depth above the test area. The section was potentially buried under significantly more than the observed 7m – and this additional sedimentation may have been removed by erosion during the Holocene (last 12 ka). Unquantified post-glacial isostatic rebound during this period means that it is difficult to constrain the thickness of any sediment removed, but there is certainly sufficient potential overburden (ice and/or sediment) to account for a degree of over-consolidation at the test site.

### 3.2 Petrographic Analysis

Thin sections were prepared from samples at four depths (1.75m, 4.5m, 7.7m and 11.9m) within the studied section and optical petrography was used to assess both mineralogy and grain morphology. The sand fraction is dominated by highly angular fragments of quartz (Figure 3).

The sand is also comprised of a significant calcite component, both as fragments of spar and as fine-grained micritic mud (presumably derived from nearby limestone bedrock). Subordinate minerals present include feldspar and minor muscovite mica – consistent with derivation from a granitic source. A matrix of clay mineral pervades the interstices and coats the framework grains (Figure 3a). The topmost sample at 1.75m includes the highest clay content, with deeper samples appearing to have less clay. However, this apparent correlation between clay content and depth is unlikely to be consistent throughout the whole section. Rather, the clay content is likely to vary on a smaller scale than the

sampling interval, reflecting the inherently laminated nature of the section and transitions between medium and fine-grained sediments. Framework grains appear fractured to varying degrees. This is especially apparent in the quartz fraction (Figure 3c). The degree of fracturing also appears to vary at the different sampling levels (Figure 3b, c).

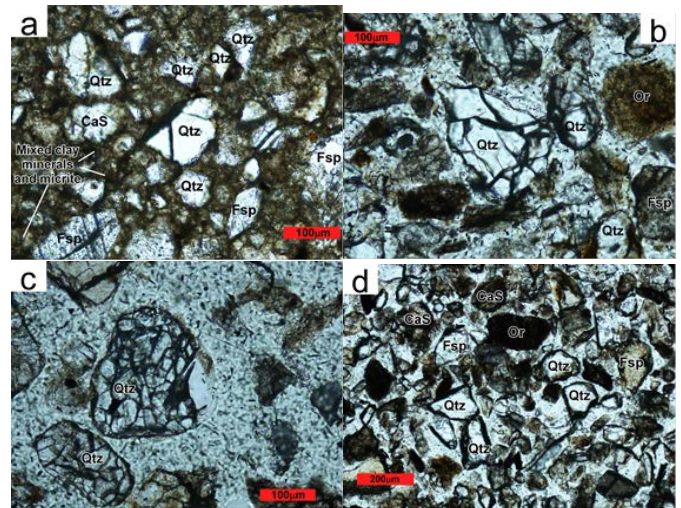


Figure 3. Photomicrographs, in plane polarized light, of samples from a) 1.75m; b) 4.5m; c) 7.7m and d) 11.9m.. Qtz = quartz, fsp = feldspar, CaS = calcite spar, Or = organic material.

### 3.3 Microstructure from SEM Imagery

A scanning electron microscope was used to investigate the micro-structure of the particles. To gather high resolution images, samples were prepared using carbon tab mounting studs and the thin sections described previously in Section 3.2.. The observed samples showed a mixture of larger particles surrounded by smaller particles, with the proportion of fine particles varying with depth. The variation in particle size within a given sample is illustrated in Figure 4.

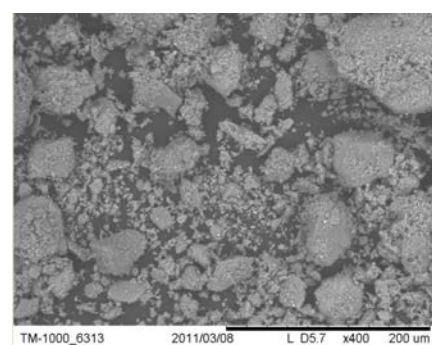


Figure 4. Sand particle matrix.

The large particles appear to be highly fractured, making them very coarse. However, the edges of the particles are still sharp rather than rounded. This means that the particles have a low sphericity but a high level of roughness. The angularity of the particles is very high. These features are illustrated in Figures 5, 6 and 7.

At smaller scales, the particles tended to appear similar to larger particles suggesting that they are particles of rock flour

that had broken away from larger (parent) particles. However, some samples contained plate-like particles of clay minerals, which were shown to be kaolinite (see Figure 8). For the most part, the sand grains were consistent with clean quartz sand as observed by the conchoidal fracture patterns (see Figure 9). This mineralogy was confirmed using X-ray diffraction analysis (XRD), which showed that the majority of particles were composed of pure silica and could be identified as quartz material.

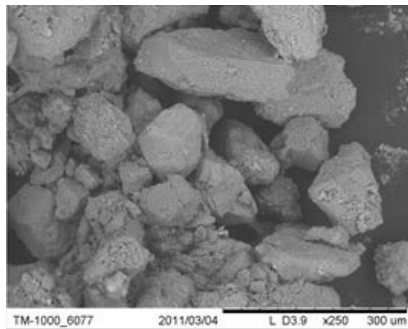


Figure 5. Sand shows high angularity but low sphericity.

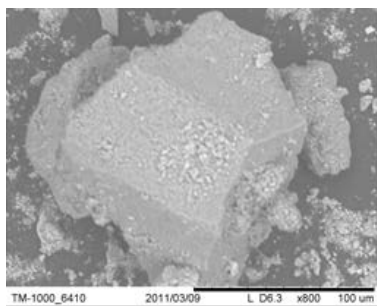


Figure 6. Individual sand grain.

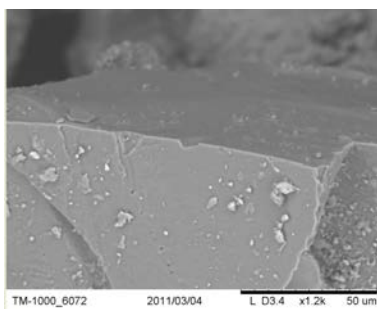


Figure 7. Clean edges on sand grain.

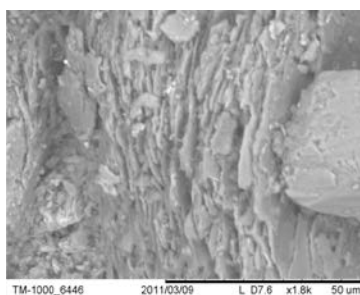


Figure 8. Clay minerals observed within fines fraction.

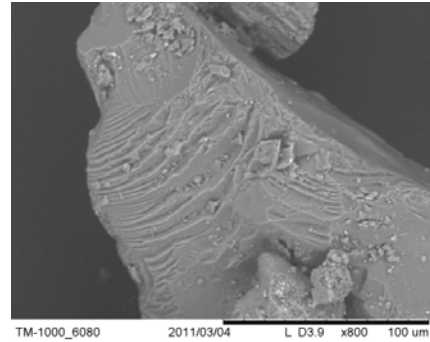


Figure 9. Conchoidal fracture pattern.

Highly angular and fractured particles were observed at all depths. The only difference in depth-dependent variation is the quantity of fines in the sample. This was apparent from macroscale observations from the site, where depositional lenses are present as shown in Figure 2. This observation was also visible in the petrographic and SEM imagery. Particle size analysis was undertaken by dry sieving as shown in Figure 10, where the percentage fines is shown to vary from 4% to 13%. The variation in fines content can be attributed to the mechanism by which the deposit formed – i.e. a glacial delta complex. During periods of high flow rates, fewer fines were deposited to the lake bed, and vice versa.

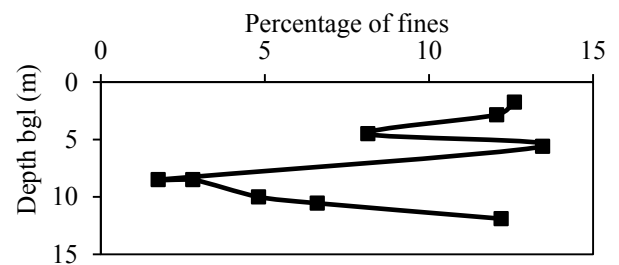


Figure 10. Fines content.

SEM imagery and XRD analysis suggest that the fines are either calcium (limestone rock flour) based or composed of pure silica (quartz), although some clay-like profiles were observed. This also agrees with the petrographic analysis of the mineralogy of the samples. The variation in clay content was also apparent in the samples taken from sonic coring, which showed large variations in cohesion. Notably, the sample taken at 1.75m depth retained excellent cohesion indicating a high level of clay and silt as shown by Figure 11.



Figure 11. Sample from 1.75m depth. Diameter of sample roughly 100mm.

4 IN-SITU TESTING

4.1 CPT Tests

Fifteen Cone Penetration Test (CPT) soundings were performed at the site by InSitu Ground Investigation Ltd. The CPT soundings were taken in a grid pattern at regular intervals across the test site to depths of between 10m and 14m. The CPT cone end resistance traces,  $q_c$  (see Figure 12), show  $q_c$  values that increased from 10MPa at the ground surface to 25MPa at 10m depth. Such large  $q_c$  values suggest a very dense deposit. The sleeve friction values from the cone,  $f_s$ , also increased with depth and the resulting friction ratio,  $F_r$ , was typically between 1% and 3%. The CPT values allowed the Blessington deposits to be classified using the Robertson [6] classification chart as a clean to silty dense sand. This agrees with the visual observations from the SEM analysis which showed mostly clean sand with smaller silty size particles.

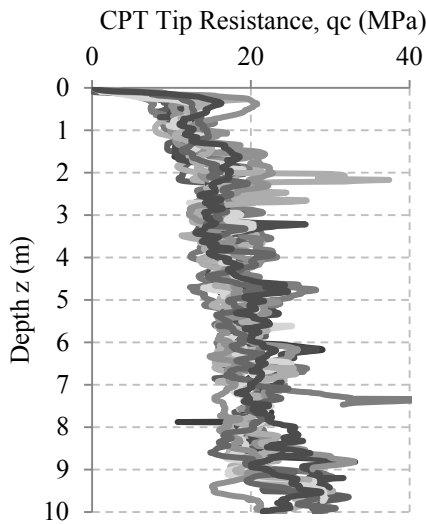


Figure 12. CPT tip resistance. Dilatometers.

Dilatometer tests performed at the site involved pushing a blade cell into the underlying sand and pausing every 250mm in order to undertake lateral expansion of the cell face (comprised of a flexible membrane) to a displacement of 1.1mm. The pressures required to initiate the expansion (the lift-off pressure  $p_0$ ) and also to generate the final strain level (the limit pressure,  $P_L$ ) were recorded, see Figure 13.

The dilatometer soundings terminated at 6m depth as the force required to advance the spade below this depth exceeded the 20t reaction force available from the CPT truck. The lift-off pressure,  $P_0$ , increased with depth from 500kPa at shallow soundings to greater than 1000kPa at 6m depth. The limit pressure showed similar increases with depth from 2MPa at 0.5m depth to 4MPa at 6m depth.

The high lateral pressures required to expand the cell at such shallow depths is indicative of high lateral earth pressures resulting from past over-consolidation. This observation ties into the geological history of the area which suggests that past layers of soil above the current ground level were removed by erosion in the past 12ka, leaving behind an over-consolidated soil mass.

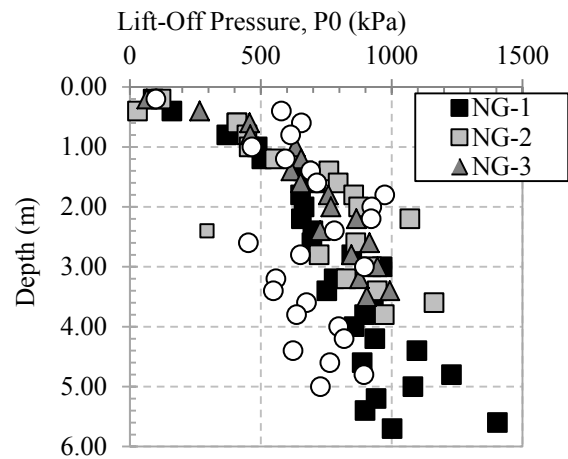


Figure 13(a). Dilatometer lift-off pressure.

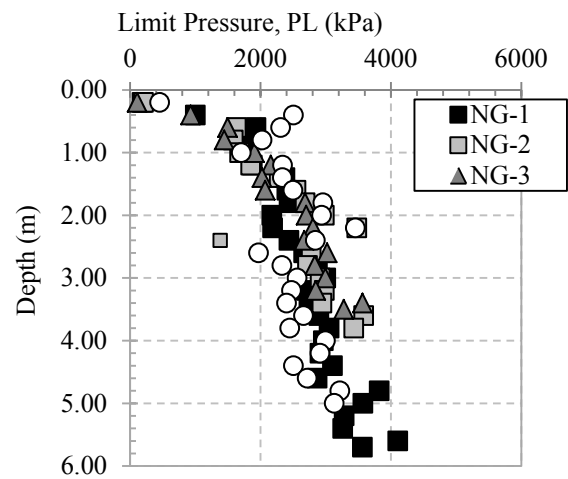


Figure 13(b). Dilatometer limit pressure.

5 OVERCONSOLIDATION

5.1 Oedometer Testing

The sonic coring procedure resulted in relatively intact cores which allowed laboratory testing to be undertaken on trimmed samples. Oedometer tests were performed on samples retrieved from depths of between 1.75m and 14m. A typical loading and unloading response is shown in Figure 14, where the void ratio is seen to decrease from an initial value of 0.17 to a final value of 0.06 under an applied vertical stress of approximately 4MPa.

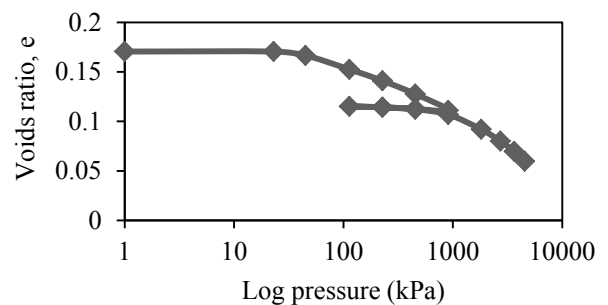


Figure 14. 1-D compression behaviour.

Using the Cassagrande method, the pre-consolidation stress was estimated to range between 600 and 1000 kPa. The resulting overconsolidation ratios (OCR) are plotted in Figure 15 as a function of depth, where a decrease from OCR = 15 at 1m depth to approximately 5 at 5m depth is observed, after which a relatively constant OCR is observed. It should be noted that there is a level of subjectivity in using the Cassagrande method to determine the pre-consolidation pressure as readings must be taken from a log scale and points selected through judgement rather than an exact algorithm.

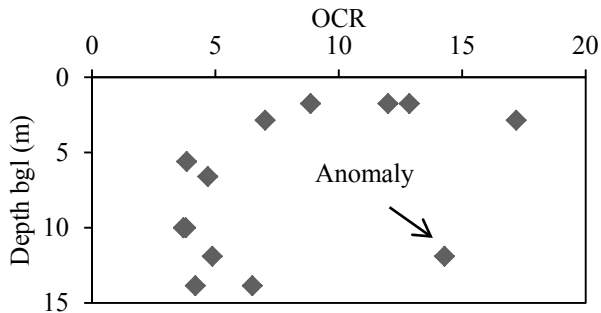


Figure 15. OCR determined from Oedometer Tests.

5.2 OCR Correlations

Because of issues such as sampling disturbance, specimen preparation and apparatus compliance at low strain levels, there is a high degree of uncertainty associated with the laboratory-determined OCR profile.

Correlations between OCR and in-situ test data determined from calibration tests on clean un-cemented un-aged quartz sands have been proposed by a number of researchers [7] [8] [9], etc. Mayne [9] proposed the following equation to determine OCR for cohesionless soils:

$$OCR = \left[ \frac{1.33q_t^{0.22}}{K_{oNC} (\sigma'_{vo})^{0.31}} \right]^{\frac{1}{(\alpha-0.27)}} \tag{1}$$

where  $q_t$  = cone tip resistance (MPa) and  $\sigma'_{vo}$  is the effective overburden pressure (kPa). The parameter  $\alpha$  can be taken as  $\alpha = (1 - K_{oNC}) \approx \sin\phi'$  for a first approximation [9]. Comparison of the CPT-determined OCR profile with the oedometer test results in Figure 16 show excellent agreement.

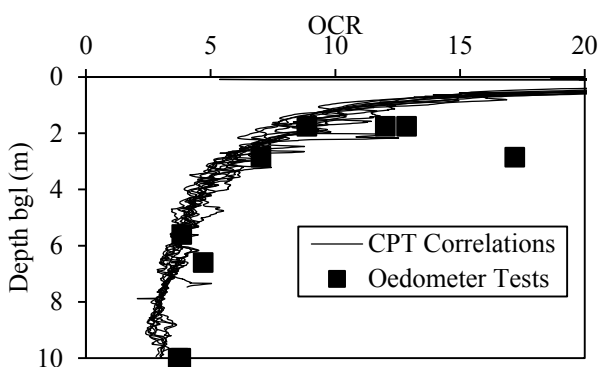


Figure 16. Comparison of OCR from CPT and oedometer data.

While correlations to predict the stress history of a deposit using dilatometer measurements are not as well established as CPT-based empirical relationships, Marchetti et al [10] have proposed a correlation from dilatometer measurements made in a study of a test embankment constructed in Venice (described in [11]). The structure was comprised of a cylindrical vertical-walled 40m diameter embankment that was kept in place for four years before being removed. The embankment loading and subsequent un-loading history were thus known, allowing a relationship between the stress history and dilatometer lift-off pressure,  $P_0$ , porewater pressure,  $u_0$  and vertical effective stress,  $\sigma'_{vo}$  to be established for the site:

$$OCR = 1.6454 \ln(K_D) - 0.3693 \tag{2a}$$

$$\text{where : } K_D = (P_0 - u_0) / \sigma'_{vo} \tag{2b}$$

The OCR profiles for the Blessington test site determined from the dilatometer correlation above are shown in Figure 17, where it is seen that OCR decreases slightly from 5 at the ground surface to 3.5 at 5m depth.

At shallow depths, the dilatometer-determined OCR values were significantly lower than those suggested by the oedometer test data and CPT correlations.

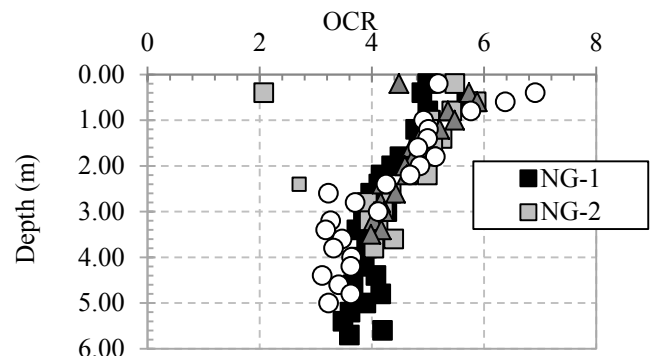


Figure 17. OCR determined from dilatometers.

6 FRICTION ANGLE

6.1 Friction Angle from Lab and Field Testing

Tolooiyan and Gavin [12] report the results of triaxial compression tests on samples of Blessington sand reconstituted at the in-situ relative density ( $\approx 100\%$ ). These revealed that the sand has a constant volume friction angle,  $\phi'_{cv}$  of  $37^\circ$  and a peak friction angle,  $\phi'_p$  which decreased from  $54^\circ$  to  $42^\circ$  for stress levels corresponding to depths ranging from 1 m to 5 m below the ground surface.

The residual friction angle measured in ring shear tests performed in the Bromhead apparatus at the appropriate effective stress level and stress history are shown in Figure 18. The soil-on-soil residual friction angle (analogous to a critical state friction angle) ranged between  $39^\circ$  and  $31^\circ$ , with an average value of  $36^\circ$ . This is in keeping with estimates for  $\phi'_{cv}$  based on the soil grading and mineralogy after Stroud [13], for a uniform highly-angular silica sand. It also agrees very well with the constant volume friction angle measured by Tolooiyan and Gavin [12].

The sand-steel residual friction angle determined in the ring shear tests using a rough steel interface produced similar



values to the soil-soil tests, suggesting minimal influence of the rough interface.

Interface ring shear tests using a smooth steel interface similar to those used to construct model piles tested at the site (see [14]) mobilised residual friction angles of 30°. This high residual friction angle can be explained by the angular edges of the sand particles as observed by the SEM.

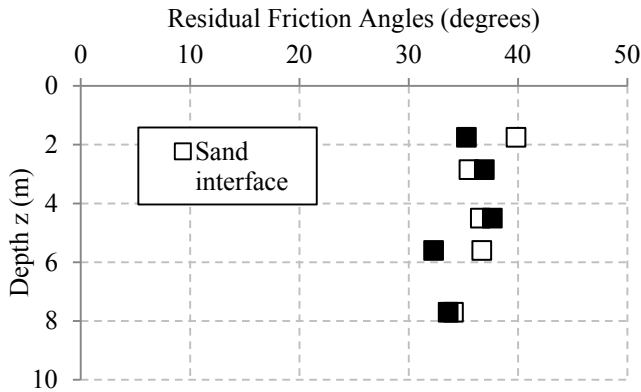


Figure 18. Residual stress friction angle.

The peak friction angle  $\phi'_p$  can be estimated from correlations with the CPT  $q_c$  values, e.g. Robertson and Campanella [15] or more recently, Kulhawy and Mayne [16]:

$$\phi' = 17.6 + \log \left( \frac{(q_c - \sigma_{v0})}{\sigma_{v0}} \right) \quad (3)$$

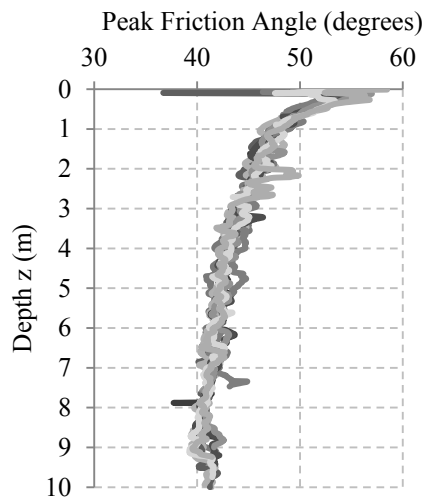


Figure 19. Peak friction angles determined from CPT resistance.

The friction angles determined from the CPT correlations (Figure 19) ranged from 55° at very shallow depths (and corresponding low effective stresses) to approximately 40° at 10 m depth is broadly in keeping with values reported from the triaxial tests performed by Tolooyan and Gavin [12].

## 7 CONCLUSIONS

This paper presents site investigation results determined from laboratory and in-situ testing at a geotechnical research site at Blessington. The following should be noted:

1. The in-situ sand is very dense and heavily over-consolidated, with high mean stress levels, which were confirmed by both in-situ and laboratory tests.

2. Peak friction angles were observed to decrease with depth from over 50° at ground surface to 40° at 10m depth. The constant volume friction angle was 36°. In interface shear tests using rough steel interfaces (comparable for example to mild steel piles), the mobilised friction angle was comparable to the soil-soil constant-volume friction angle.
3. Field testing (and in particular the CPT test) was shown to provide excellent correlations with laboratory estimates of the stress and strength characteristics of the deposit.

## ACKNOWLEDGMENTS

The authors wish to express their gratitude to Mainstream Renewable Power, the Irish Research Council for Science and Technology (IRCSET), Science Foundation Ireland (through grant number 10-RFP-GEO2895) and Enterprise Ireland for co-financing these field tests. In addition, the authors wish to thank Irish Geotechnical Services (IGSL) and Boart Longyear for performing the sonic coring and Martin Carney at TCD for assisting with the ring shear tests.

## REFERENCES

- [1] Igoe D. (2010) *Offshore Foundations: A comparison of full-displacement and partial displacement piles in sand*, PhD Thesis, University College Dublin
- [2] Syge, F.M. (1977) *West Wicklow*, In South-East Ireland International Union of quaternary research field guide, Vol.56
- [3] Coxon, P., 1993. Irish Pleistocene biostratigraphy. *Irish Journal of Earth Sciences*, 12,83-105.
- [4] Doherty P. and Gavin K. (2010) "Statistical use of CPT data and implications for pile design" *Proc. Of the 2<sup>nd</sup> International Conference on Cone Penetration Testing*
- [5] Philcox, M.E., 2000. The glacio-lacustrine delta complex at Blessington, Co. Wicklow and related outflow features. In: *Guidebook of the 20th Regional Meeting of the International Association of Sedimentologists*, Graham, J.R and Ryan, A. (eds). Trinity College Dublin. 129-152.
- [6] Robertson (1990) Soil Classification using the CPT *Canadian Geotechnical Journal*
- [7] Mayne, P.W. (1995). CPT determination of OCR and  $K_0$  in clean quartz sands. *Proceedings, Symposium on Cone Penetration Testing*, Vol. 2, Swedish Geotechnical Society, 215-220.
- [8] Lunne, T., Robertson, P.K., & Powell, J.J.M. (1997). *Cone Penetration Testing in Geotechnical Practice*, Blackie Academic & Professional, Chapman and Hall, London, 312 p.
- [9] Mayne, P.W. (2001). Stress-strain-strength-flow parameters from enhanced in-situ tests. *Proceedings, Intl. Conf. on In-Situ Measurement of Soil Properties & Case Histories*, Bali, Indonesia, 27-48.
- [10] Marchetti et al (2012) "Overconsolidation and stiffness of Venice lagoon sands from SDMT and CPTU" *ASCE Jnl GGE*, in press.
- [11] Marchetti, S., P. Monaco, M. Calabrese & G. Totani (2006) Comparison of moduli determined by DMT and back figured from local strain measurements under a 40 m diameter circular test load in the Venice area. *Proc. From the second international flat dilatometer conference*
- [12] Tolooyan, A. and Gavin, K.; (2011) 'Modelling the Cone Penetration Test in sand using Cavity Expansion and Arbitrary Lagrangian Eulerian Finite Element Methods'. *Computers and Geotechnics*, 38 (4):482-490
- [13] Stroud M. A (1974) The standard penetration test in insensitive clays and soft rocks. *Proc. Of the European Conference on Penetration Testing*. Vol 2(2) Stockholm 367-375
- [14] Gavin, K.G, Igoe, D.I and O'Kelly, B. The effect of soil state on the shaft capacity of piles in sand, *paper submitted to ASCE Journal of Geotechnical and Geoenvironmental Engineering*
- [15] Robertson, P.K., and Campanella, R.G., 1983. Interpretation of cone penetration tests – Part I (sand). *Canadian Geotechnical Journal*, 20(4): 718-733.
- [16] Kulhawy, F.H., and Mayne, P.H., 1990. *Manual on estimating soil properties for foundation design*, Report EL-6800 Electric Power Research Institute, EPRI, August 1990.